PROCEEDINGS OF THE ROYAL SOCIETY B

rspb.royalsocietypublishing.org

Research

Cite this article: He D, Dushoff J, Eftimie R, Earn DJD. 2013 Patterns of spread of influenza A in Canada. Proc R Soc B 280: 20131174. http://dx.doi.org/10.1098/rspb.2013.1174

Received: 10 May 2013
Accepted: 16 August 2013

Subject Areas:
health and disease and epidemiology

Keywords:
influenza, spatial pattern, weather, pandemic, school term, vaccination

Author for correspondence:
Daihai He
e-mail: hedaihai@gmail.com

Electronic supplementary material is available at http://dx.doi.org/10.1098/rspb.2013.1174 or via http://rspb.royalsocietypublishing.org.

Royal Society Publishing
Informing the science of the future

Patterns of spread of influenza A in Canada

Daihai He[1], Jonathan Dushoff[2,3], Raluca Eftimie[4] and David J. D. Earn[3,5]

[1]Department of Applied Mathematics, Hong Kong Polytechnic University, Hung Hom, Kowloon, Hong Kong (SAR), People's Republic of China
[2]Department of Biology, and [3]M.G. DeGroote Institute for Infectious Disease Research, McMaster University, Hamilton, Ontario, Canada L8S 4L8
[4]Division of Mathematics, University of Dundee, Dundee DD1 4HN, UK
[5]Department of Mathematics and Statistics, McMaster University, Hamilton, Ontario, Canada L8S 4K1

Understanding spatial patterns of influenza transmission is important for designing control measures. We investigate spatial patterns of laboratory-confirmed influenza A across Canada from October 1999 to August 2012. A statistical analysis (generalized linear model) of the seasonal epidemics in this time period establishes a clear spatio-temporal pattern, with influenza emerging earlier in western provinces. Early emergence is also correlated with low temperature and low absolute humidity in the autumn. For the richer data from the 2009 pandemic, a mechanistic mathematical analysis, based on a transmission model, shows that both school terms and weather had important effects on pandemic influenza transmission.

1. Introduction

Seasonality of transmission rates is known to have a significant influence on the temporal patterns of epidemics of infectious diseases [1]. Transmission rates appear to be influenced both by contact patterns (e.g. aggregation of children in schools when schools are in session [2–5]) and by weather patterns (e.g. changes in humidity and/or temperature [5–10]). Understanding how these factors—and others, such as travel patterns—affect the full spatio-temporal dynamics of infectious disease spread is important for epidemic prediction and control.

The spatial spread of influenza across countries and continents has become a very active area of research [11–15], and recent work has begun to connect transmission mechanisms with observed spatial patterns. In particular, influenza mortality patterns across the continental United States are correlated with differences in absolute humidity [7]. Here, we investigate the relationships among weather variables (temperature and humidity), school calendars and influenza incidence across the 10 Canadian provinces over the last 14 years. We use statistical models to investigate correlations over this period, and in the case of the 2009 pandemic, we also fit mechanistic mathematical models that allow us to draw stronger conclusions about the effects of seasonal factors on influenza transmission and incidence.

2. Material and methods

(a) Data sources

Weekly influenza A laboratory-confirmed cases between 23 October 1999 and 9 March 2013 were taken from the Public Health Agency of Canada FluWatch surveillance programme reports [16]. Daily climate data were obtained from Canada's National Climate Archive [17]. We used climate data for the most populous city in each province to represent the province. School opening and closing dates were obtained from the Canadian Education Association (http://www.cea-ace.ca/); if these dates were not uniform throughout a province, we averaged the published dates.

Population sizes and estimated pandemic H1N1 (pH1N1) vaccination coverage in each of the 10 Canadian provinces in 2009 and 2010 were obtained from Statistics

Canada [18,19]. In Toronto (Ontario, ON) and Montreal (Quebec, QC), the majority of vaccine doses were delivered during November and December [20,21]. Since vaccination dates were not available for other provinces, we assumed that they also vaccinated during the same time span.

(b) Statistical analysis: generalized linear model

We looked for patterns in influenza epidemic timing for the 11 seasonal influenza (nine pre-pandemic and two post-pandemic) seasons in our dataset. Each flu season starts from the 35th week of each year and testing occurs throughout the year in Canada [16]. To avoid spurious findings, we restricted ourselves to a single set of predictors specified *a priori* in the main analysis:

— spatial ordering of provinces from east to west (longitude rank),
— population rank of the provinces (population rank),
— mean observed October humidity, and
— mean observed October temperature.

To facilitate an unambiguous ranking of longitude (see geographical locations of the 10 Canadian provinces in the electronic supplementary material), we grouped Canada's four Atlantic provinces into one 'mega-province'. Thus, our analysis treated seven regions of Canada (six provinces and one mega-province).

To test the significance of our hypotheses, we used the R statistical programming language (http://www.R-project.org/) to model epidemic timing as a function of the four predictors. We also considered influenza season (treated categorically) to account for the fact that overall timing was different in different years. Our measure of epidemic timing was the date on which the number of cumulative cases reported reached a given proportion of the seasonal total for a given season in each province, which we call the *quantile time*. To test whether a set of predictors is significant as a group, we used an analysis of variance test to compare the original model to a model that excludes the focal predictors.

(c) Mathematical model and data fitting

To connect seasonal factors with influenza transmission during the autumn wave of the 2009 pandemic (4 July 2009 to 18 December 2009), we used a standard mechanistic mathematical model, the classical SIR model [1]

$$\dot{S} = -\beta(t)SI - v(t), \tag{2.1a}$$

$$\dot{I} = \beta(t)SI - \rho\gamma I - (1-\rho)\gamma I. \tag{2.1b}$$

Here, S and I represent the numbers of susceptible and infectious individuals, γ is the recovery rate (the rate at which individuals move from the infectious class to the recovered class), and we assumed that the mean infectious period (γ^{-1}) is 3 days [5,22–25]. ρ is the reporting ratio (the proportion of cases that are reported). $v(t)$ is the vaccination rate. We define

$$v(t) = \begin{cases} \dfrac{\eta\phi S(0)}{D}, & t \in (10\,\text{October}\,2009,\ 10\,\text{January}\,2010) \\ 0, & \text{otherwise.} \end{cases} \tag{2.2}$$

where η denotes the vaccine effectiveness, $\eta = 66\%$ [26]; ϕ denotes the vaccination coverage and the estimation is available for each province [19]; $S(0)$ denotes the initial susceptibles; D denotes the duration of the vaccination campaign, which was approximately two months. The vaccination campaign was started in the last week of October 2009 [20]. We assume that the vaccination became effective between (10 October 2009 and 10 January 2010), to allow for the delay in vaccine-induced protection [26].

Testing was restricted for a substantial portion of the 2009 pandemic, so the reporting ratio ρ was not constant throughout the epidemic. However, restrictions were initiated before our analysis period started in July [27], allowing us to use a constant ρ—with the exception of Alberta, where testing was not restricted until November [5]. Hence we used a step function for ρ in Alberta.

In equations (2.1*a*,*b*), the transmission rate β is time-varying (dependent on weather and the school calendar). We took it to have the following specific form:

$$\beta(t) = \beta_0 \cdot e^{-\alpha_H H(t)} \cdot e^{-\alpha_T T(t)} \times \begin{cases} 1, & \text{summer vacation,} \\ 1+\varepsilon, & \text{school term.} \end{cases} \tag{2.3}$$

Here, $H(t)$ is the absolute humidity and $T(t)$ is the temperature at time t. The parameter β_0 is the baseline transmission rate during the summer vacation. The parameter ε, which we call the *school term intensity*, controls the increment in transmission after schools reopen in September. The parameters α_H and α_T describe the strength of response to humidity and temperature, respectively. This definition of $\beta(t)$ gives us $2^3 = 8$ scenarios to consider, since we can separately turn off the effects of school terms, temperature or humidity. Below we focus on the following three 'sub-models': (i) only school terms and temperature ($\alpha_H = 0$), (ii) only school terms and humidity ($\alpha_T = 0$) and (iii) only school terms ($\alpha_T = \alpha_H = 0$).

Because temperature and humidity are highly correlated, and the functional responses are imperfectly known, we do not expect to be able to disentangle the separate contributions of these two factors. We therefore do not analyse any models that incorporate both humidity and temperature.

In our simulations, we assumed that the initial proportion of susceptible individuals $S(0)/N$ was 65% (on 4 July 2009; in the electronic supplementary material, we investigate two other assumptions for this quantity), and the initial proportion of infected individuals was below 1% (cf. [28–31]). We define the basic reproduction number $\mathcal{R}_0 = \langle\beta(t)\rangle/\gamma$ [32], where the expectation is taken over the time window that we model. We also define the effective reproduction number $\mathcal{R}_e = \mathcal{R}_0 S(0)/N$.

3. Results

(a) Patterns of annual influenza epidemic spread across Canada

Figure 1*a* shows the weekly laboratory-confirmed influenza A cases for each Canadian province from October 1999 to March 2013 (the last few months are not included in our analysis, since we do not have complete data for this flu year). The top axis indicates which subtype was most common in each season. Epidemics tended to begin earlier in the H3N2-dominated seasons. In addition, three provinces (British Columbia (BC), Alberta (AB) and ON) tended to have earlier influenza epidemics than the rest of Canada.

Figure 1*b–d* shows the times at which 25, 50 and 75% of weekly laboratory-confirmed cases occurred in the non-pandemic years (i.e. excluding the 2009–2010 and 2010–2011 flu years). Figure 1*b* suggests that on average, influenza tends to start earliest in AB, followed by BC and ON, eventually reaching the Maritimes (MA) last. There is much less evidence of spatial spread when we look later in the seasons (figure 1*c*,*d*). Figure 1*e* shows the temperature pattern, which may explain why flu starts in BC later than in AB; humidity (not shown here) follows a similar pattern. We use the Tukey-

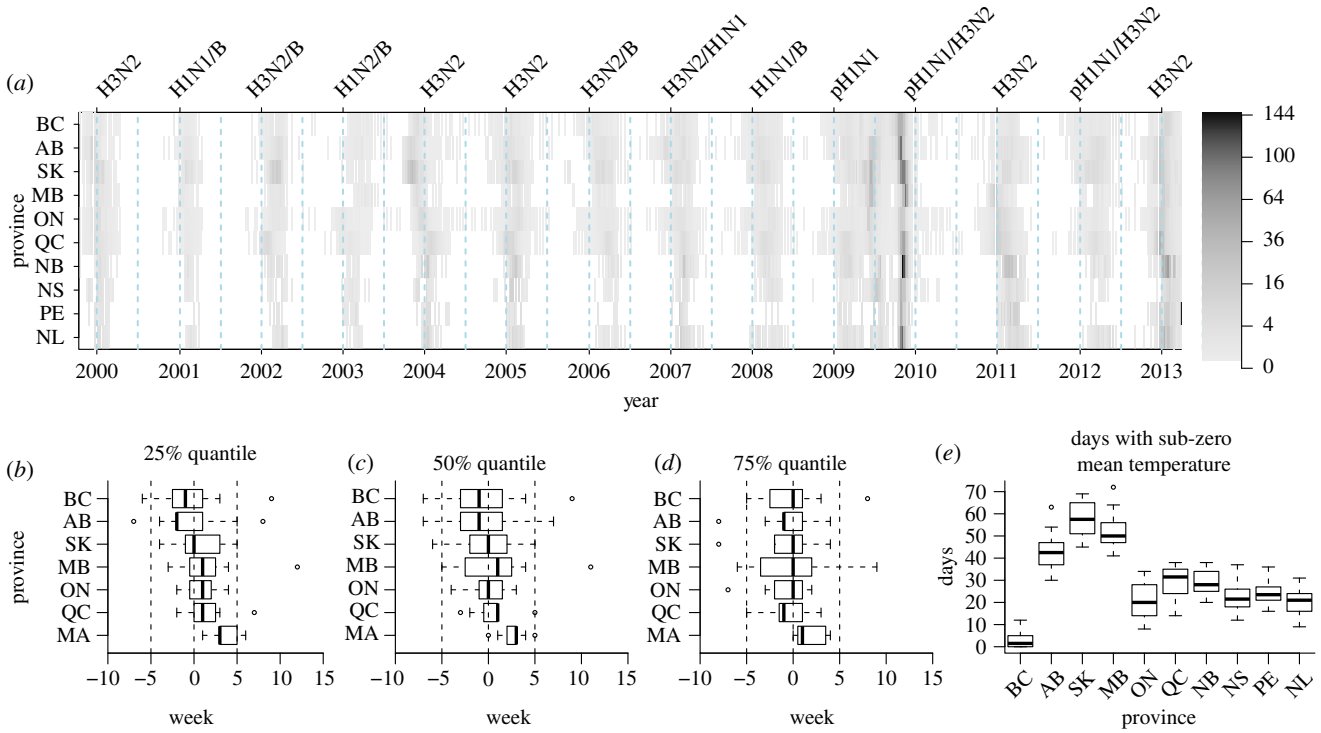

Figure 1. Spatio-temporal pattern of influenza A transmission in Canada. (*a*) Weekly laboratory-confirmed influenza A cases in the 10 Canadian provinces (per 100 000 habitants) from October 1999 to March 2013. Labels at the top show the dominant subtype(s) in Canada in each influenza season [16]. Vertical dashed lines are shown on 1 January and 1 July of each year. (*b–d*) Deviations of the provincial quantile times (at 25, 50 and 75%) from corresponding Canadian quantile times for each year. MA here refers to the Maritime provinces of NB, NS, PE and NL. (*e*) The number of days (between September and December, for each year between 1999 and 2012) when the mean temperature was below zero. Provinces are ordered in longitude order from west to east (see the electronic supplementary material, figure S4). (Online version in colour.)

style *boxplot* in R (http://stat.ethz.ch/R-manual/R-patched/library/grDevices/html/boxplot.stats.html) in figure 1*b–e*.

Using a generalized linear model controlling for the effect of variation among influenza seasons (see Material and methods), we analysed the roles of four predictors: longitude rank, population rank, humidity and temperature. We are mostly interested in the initial spreading, thus we used 25% as the threshold proportion (we show other cases in the electronic supplementary material). We found that all four predictors as a group are significant ($p \approx 0.001$). In particular, longitude rank, humidity and temperature are significant individually ($p < 0.001$, 0.021 and 0.016, respectively). Although population is not a significant predictor ($p = 0.413$), a direct comparison between longitude rank and population rank does not show that the former is significantly *better* than the latter.

(b) Pattern of 2009 pandemic spread across Canada

Recent work has indicated that school closures lead to a significant reduction in transmission of influenza (e.g. seasonal influenza in France [33] and pandemic influenza in the province of AB, Canada [5]). Figure 2 suggests that summer closings of schools in 2009 influenced the transmission dynamics of pandemic influenza throughout Canada and led to substantially fewer cases during the summer months than would have occurred if schools had remained open all summer. The figure reveals a variety of suggestive patterns: for example, provinces that closed schools earlier (e.g. QC) seem in general to have experienced fewer cases, whereas provinces that opened schools earlier (e.g. AB and Saskatchewan (SK)), seem to have experienced an earlier second wave. However, the pattern of autumn spread also seems broadly consistent with the spatio-temporal patterns of temperature and absolute humidity; in particular, a wave of low temperature (and absolute humidity) in October 2009 is correlated with the peak of the second wave of the pandemic. Also worth noting is the relatively low number of reported cases in the more populous provinces of ON and QC (probably due to testing restrictions) and many periods with very few reports from Manitoba (MB), Nova Scotia (NS), Prince Edward Island (PE) and Newfoundland (NL) between April and October 2009 (possibly indicating local fade-out and re-introduction).

To explore these patterns mechanistically, we fit an SIR model to the pandemic data (see Material and methods). Figure 3 shows the log-likelihood profiles of the three sub-models as a function of school term intensity (ε, equation (2.3)) in each of the seven regions of Canada (six provinces and the maritime 'mega-province'). Higher likelihood indicates better fit. It is evident that sub-model (i), with an additional effect of temperature variation, is the best among the three sub-models in all regions. Sub-model (ii), with humidity replacing temperature, is as good as sub-model (i) in ON and MB. Sub-model (iii), with neither weather variables, is clearly the worst in all regions. Note that sub-models (i) and (ii) involve the same number of parameters, while sub-model (iii) involves one fewer parameter. The difference between sub-model (iii) and sub-models (i) and (ii) is much more than can be explained by reducing the number of parameters by one ($\approx$4 units of log likelihood). Electronic supplementary material, table S2 shows the second-order Akaike information criterion (AIC_c) [5,8,35] for the three sub-models for each of the seven regions (AIC_c formalizes a tradeoff between model complexity and goodness of fit).

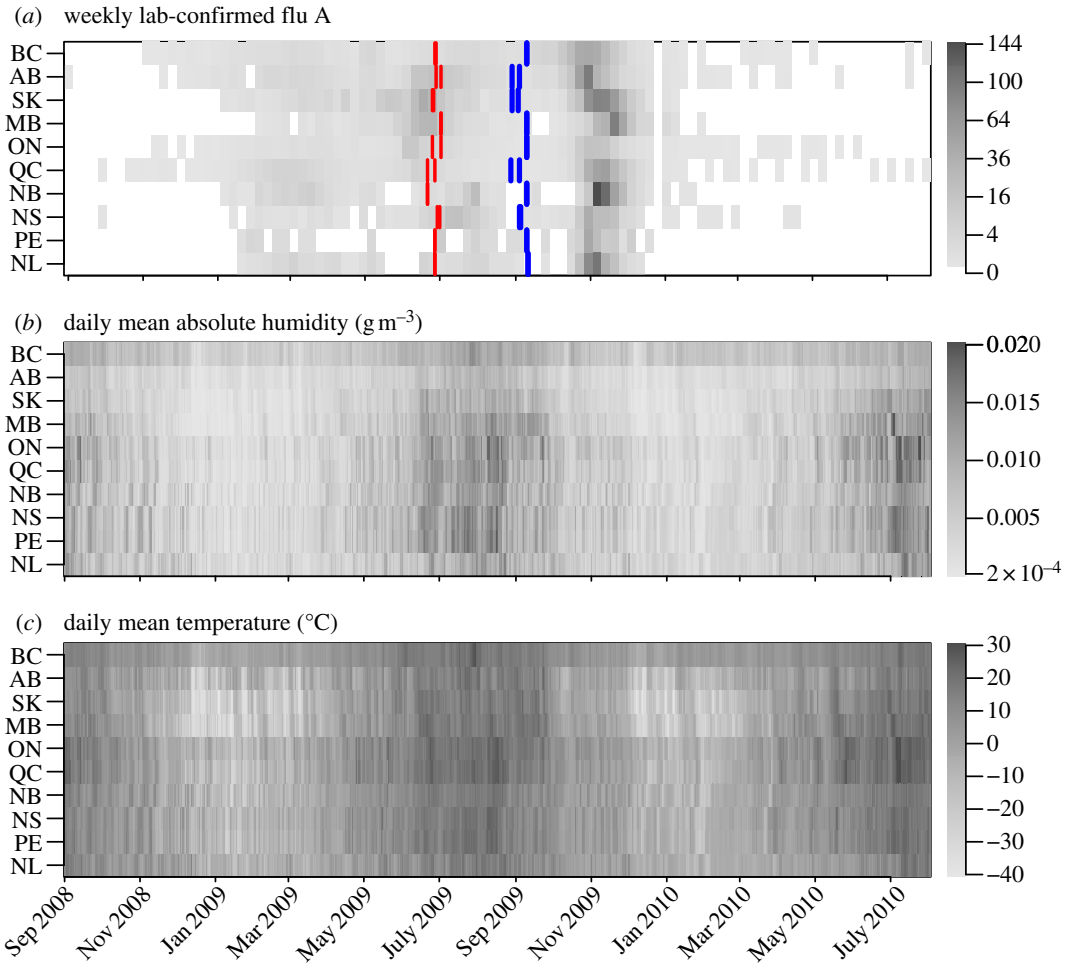

Figure 2. Spatial pattern of influenza A (mainly pandemic H1N1) transmission in Canada (*a*), as well as daily mean absolute humidity (*b*) and temperature (*c*) across all Canadian provinces, between September 2008 and July 2010. (*a*) Also shows school closing dates (the thin vertical lines in late June) and opening dates (the thick vertical lines in early September). In some provinces, there were several school closing/opening dates, corresponding to different regions and/or for different grades. (Online version in colour.)

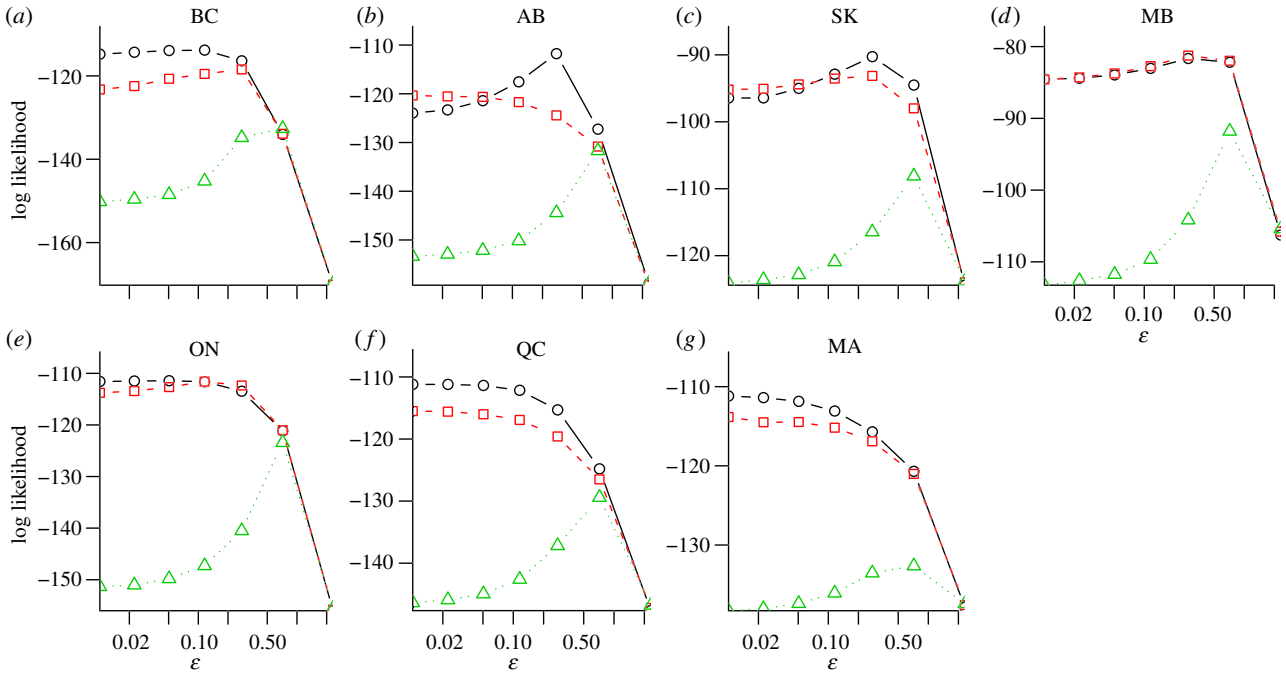

Figure 3. Likelihood profiles of three sub-models as a function of school term factor in each of the seven Canadian regions. The likelihood profile is obtained by maximizing the likelihood of each of the three sub-models while fixing the school term factor at values spanning from 0.01 to 2.3, via iterated filtering [34]. Three symbols (circle (temperature sub-model), square (humidity sub-model) and triangle (no-weather sub-model)) correspond to sub-models (i)–(iii) as defined in Material and methods. Sub-model (i), with an effect of temperature variation, is the best. Sub-model (iii), with neither weather factors, is the worst in all provinces. Comparison of their second-order Akaike information criterion is given in the electronic supplementary material. (Online version in colour.)

Table 1. The maximum-likelihood estimates of parameters for the autumn wave of the 2009 influenza pandemic in seven Canadian regions, estimated using sub-model (i), the sub-model with an effect of temperature variation. The parameters are the reproductive number, the attack rate (AR), the reporting ratio ρ, the baseline transmission rate, the temperature intensity (α_T) and the school term intensity (ε). For α_T and ε, the 95% confidence intervals (CIs) are given in parentheses.

province	R_e	AR (%)	ρ	β_0	α_T	95% CI of α_T	ε	95% CI of ε
BC	1.27	43.5	0.0035	374.37	0.045	(0.033, 0.054)	0.088	(0.010, 0.247)
AB	1.25	42.6	0.0054	229.48	0.028	(0.023, 0.034)	0.247	(0.180, 0.343)
SK	1.32	45.7	0.0060	229.14	0.031	(0.022, 0.039)	0.261	(0.146, 0.484)
MB	1.32	45.9	0.0033	249.63	0.037	(0.013, 0.049)	0.384	(0.083, 0.614)
ON	1.30	45.0	0.0012	406.49	0.050	(0.035, 0.052)	0.075	(0.010, 0.261)
QC	1.27	45.3	0.0034	368.04	0.046	(0.042, 0.053)	0.018	(0.010, 0.189)
MA	1.31	47.0	0.0044	411.93	0.065	(0.058, 0.077)	0.011	(0.010, 0.113)

Figure 3 also reveals a relationship between the effects of weather and school term in the data. When the school term intensity is large, the difference between sub-models with and without weather decreases; whereas when the school term intensity is small, sub-models that include weather fit the data much better than those that include neither weather variable. These observations suggest that the effects of school term and weather variation are similar. We also note that the likelihood profiles for the prairie provinces (AB, SK and MB) have similar shapes, perhaps due to the proximity in geography and similarity in climate among these provinces. The 95% CIs for the school term intensity can be calculated from figure 3 via the procedure described in [36].

Table 1 shows our maximum-likelihood estimates of parameters: the reproductive number ($\mathcal{R}_e$), the attack rate (AR, the total infected proportion), the baseline transmission rate (β_0), the temperature intensity and the school term intensity (ε), in each of the seven regions, based on sub-model (i). The $\mathcal{R}_e$ estimates for the autumn pandemic wave are close to published estimates for the spring wave [5,23–25]. Our estimated ARs are larger than published values, e.g. 36% published in [37] (for the whole pandemic including vaccination). However, the published values were based on haemagglutination inhibition (HI) titres greater than or equal to 40; if a lower threshold (greater than or equal to 20) is used, the estimated AR is larger [30,37].

Electronic supplementary material, figures S9 and S10, compare the observed data with simulations with estimated parameter values for the three sub-models in each of the seven regions. It can be seen that simulations without weather variables match the observed data less well than those that include weather variables.

Electronic supplementary material, figure S7, shows total number of laboratory-confirmed influenza cases in each region during the pandemic year (with a box plot of annual cases during pre-pandemic seasonal epidemics for comparison), the reporting ratio and the school term intensity (with 95% confidence interval), estimated from the three sub-models for the pandemic year. The results show that the sub-model without temperature or humidity gives higher estimates of reporting ratio and school term intensity.

4. Discussion and conclusion

In this article, we have reported evidence of a west-to-east spatial pattern of spread of seasonal influenza A across Canada between 1999 and 2013, using a simple statistical model. We also studied the autumn wave of the 2009 pandemic in more detail, using a model with explicit transmission, which allowed us to demonstrate that the spread of influenza across Canada is strongly affected by weather even when school terms are accounted for. For seasonal influenza, we demonstrated that longitude rank, humidity and temperature are significant predictors. We chose not to fit a mechanistic model to the seasonal influenza data, since seasonal influenza tends to be sampled more poorly, and the data generally include multiple strains.

Our results on the pattern of seasonal epidemic spread are consistent with an earlier phenomenological report that covered both the USA and Canada [15]. Our results on the importance of weather in pandemic transmission are consistent with similar observations across the United States for seasonal influenza [7].

This study aggregated cases at the provincial level and did not distinguish between age groups. This allowed us to obtain robust fits, but may have led us to miss some details. The aggregated fits also complicate the interpretation of our school term effect. The direct effect of school terms on transmission among schoolchildren will be greater than our estimated effect, averaged over the whole population. Quantifying this difference would require an understanding of the extent to which schoolchildren drive the influenza epidemic, both when schools are open and when they are closed, which in turn would require an age-structured model.

In the electronic supplementary material, we also investigated the timing of intervention and showed its importance on the reduction of infections. While this study is not the first one to investigate vaccination measures in Canada during the 2009 pandemic (see [38]), it is the first that includes the effects of weather. Overall, our study suggests that better understanding of the factors underlying patterns of spatio-temporal spread will be very useful for designing and prioritizing vaccination and other control efforts. As influenza surveillance and modelling techniques continue to improve, it should become possible to further unravel the climate factors that affect influenza transmission using data from seasonal epidemics.

Acknowledgements. We thank two anonymous referees for helpful comments on the manuscript. The authors thank Dr Joseph Wu and Mike Delorme for helpful discussion.

Funding statement. J.D. and D.J.D.E. were supported by grants from CIHR and NSERC. D.H. was supported by a start-up grant from the Department of Applied Mathematics at Hong Kong Polytechnic University (HKPU) and an HKPU 'Central Bidding' grant.

References

1. Anderson RM, May RM. 1991 *Infectious diseases of humans: dynamics and control*. Oxford, UK: Oxford University Press.
2. London W, Yorke JA. 1973 Recurrent outbreaks of measles, chickenpox and mumps. I. Seasonal variation in contact rates. *Am. J. Epidemiol.* **98**, 453–468.
3. Olsen LF, Schaffer WM. 1990 Chaos versus noisy periodicity: alternative hypotheses for child-hood epidemics. *Science* **249**, 499–504. (doi:10.1126/science.2382131)
4. Earn DJD, Rohani P, Bolker BM, Grenfell BT. 2000 A simple model for complex dynamical transitions in epidemics. *Science* **287**, 667–670. (doi:10.1126/science.287.5453.667)
5. Earn DJD, He D, Loeb MB, Fonseca K, Lee BE, Dushoff J. 2012 Effects of school closure on pandemic influenza incidence in Alberta, Canada. *Ann. Intern. Med.* **156**, 173–181. (doi:10.7326/0003-4819-156-3-201202070-00005)
6. Lowen AC, Mubareka S, Steel J, Palese P. 2007 Influenza virus transmission is dependent on relative humidity and temperature. *PLoS Pathog.* **3**, e151. (doi:10.1371/journal.ppat.0030151)
7. Shaman J, Pitzer VE, Viboud C, Grenfell BT, Lipsitch M. 2010 Absolute humidity and the seasonal onset of influenza in the continental united states. *PLoS Biol.* **8**, e1000316. (doi:10.1371/journal.pbio.1000316)
8. He D, Dushoff J, Day T, Ma J, Earn DJD. 2011 Mechanistic modelling of the three waves of the 1918 influenza pandemic. *Theor. Ecol.* **4**, 283–288. (doi:10.1007/s12080-011-0123-3)
9. Makoto S, Kouki K, Kunio S. 2011 Absolute humidity as a deterministic factor affecting seasonal influenza epidemics in Japan. *Tohoku J. Exp. Med.* **224**, 251–256. (doi:10.1620/tjem.224.251)
10. van Noort SP, Aguas R, Ballesteros S, Gomes MGM. 2011 The role of weather on the relation between influenza and influenza-like illness. *J. Theor. Biol.* **298**, 131–137. (doi:10.1016/j.jtbi.2011.12.020)
11. Ferguson NM, Cummings DA, Cauchemez S, Fraser C, Riley S, Meeyai A, Iamsirithaworn S, Burke DS. 2005 Strategies for containing an emerging influenza pandemic in Southeast Asia. *Nature* **437**, 209–214. (doi:10.1038/nature04017)
12. Viboud C, Bjornstad ON, Smith DL, Simonsen L, Miller MA, Grenfell BT. 2006 Synchrony, waves, and spatial hierarchies in the spread of influenza. *Science* **312**, 447–451. (doi:10.1126/science.1125237)
13. Sattenspiel L. 2009 *The geographic spread of infectious diseases: models and applications*. Princeton, NJ: Princeton University Press.
14. Eggo RM, Cauchemez S, Ferguson NM. 2011 Spatial dynamics of the 1918 influenza pandemic in England, Wales and the United States. *J. R. Soc. Interface* **8**, 233–243. (doi:10.1098/rsif.2010.0216)
15. Schanzer DL, Langley JM, Dummer T, Aziz S. 2011 The geographic synchrony of seasonal influenza: a waves across Canada and the United States. *PLoS ONE* **6**, e21471. (doi:10.1371/journal.pone.0021471)
16. FluWatch. 2010 *FluWatch reports 1999/2000–2009/2010*. Public Health Agency of Canada. See http://www.phac-aspc.gc.ca/fluwatch.
17. EnvironCan. 2010 *Environment Canada—Canada's National Climate Archive*. See http://www.climate.weatheroffice.gc.ca/.
18. StatCan. 2010 *Statistics Canada—CANSIM table 051-0001*. See http://www.statcan.gc.ca/tables-tableaux/sum-som/l01/cst01/demo02a-eng.htm.
19. Gilmour H, Hofmann N. 2010 H1N1 vaccination. Statistics Canada Health Reports. 82-003-X. See http://www.statcan.gc.ca/pub/82-003-x/2010004/article/11348-eng.htm.
20. Toronto10. 2010 2009–2010 pH1N1 Influenza Pandemic Summary Report. Toronto Public Health Information for Health Professionals. See http://www.toronto.ca/health/professionals/pandemic_influenza/.
21. Delorme M. 2010 Studies on mathematical modelling of influenza in Canada. MSc Thesis, McMaster University, Canada.
22. Pourbohloul B *et al*. 2009 Initial human transmission dynamics of the pandemic (H1N1) 2009 virus in North America. *Influenza Other Respir. Viruses* **3**, 215–222. (doi:10.1111/j.1750-2659.2009.00100.x)
23. Cauchemez S, Donnelly CA, Reed C, Ghani AC, Fraser C, Kent CK, Finelli L, Ferguson NM. 2009 Household transmission of 2009 pandemic influenza A (H1N1) Virus in the United States. *NEngl. J. Med.* **361**, 2619–2627. (doi:10.1056/NEJMoa0905498)
24. Tuite AR *et al*. 2010 Estimated epidemiologic parameters and morbidity associated with pandemic H1N1 influenza. *Can. Med. Assoc. J.* **182**, 131–136. (doi:10.1503/cmaj.091807)
25. Donnelly CA *et al*. 2011 Serial intervals and the temporal distribution of secondary infections within households of 2009 pandemic influenza A (H1N1): implications for influenza control recommendations. *Clin. Infect. Dis.* **52**(Suppl. 1), S123–S130. (doi:10.1093/cid/ciq028)
26. Valenciano M *et al*. 2011 Estimates of pandemic influenza vaccine effectiveness in Europe, 2009–2010: results of influenza monitoring vaccine effectiveness in Europe (I-MOVE) multicentre case-control study. *PLoS Med.* **8**, e1000388. (doi:10.1371/journal.pmed.1000388)
27. Skowronski DM *et al*. 2011 Effectiveness of AS03 adjuvanted pandemic H1N1 vaccine: case-control evaluation based on sentinel surveillance system in Canada, autumn 2009. *Br. Med. J.* **342**, c7297. (doi:10.1136/bmj.c7297)
28. Miller E, Hoschler K, Hardelid P, Stanford E, Andrews N, Zambon PM. 2010 Incidence of 2009 pandemic influenza A H1N1 infection in England: a cross-sectional serological study. *Lancet* **375**, 1100–1108. (doi:10.1016/S0140-6736(09)62126-7)
29. Mahmud SM *et al*. 2010 Estimated cumulative incidence of pandemic (H1N1) influenza among pregnant women during the first wave of the 2009 pandemic. *Can. Med. Assoc. J.* **182**, 1522–1524. (doi:10.1503/cmaj.100488)
30. Kelly H, Peck HA, Laurie KL, Wu P, Nishiura H, Cowling BJ. 2011 The age-specific cumulative incidence of infection with pandemic influenza H1N1 2009 was similar in various countries prior to vaccination. *PLoS ONE* **6**, e21828. (doi:10.1371/journal.pone.0021828)
31. Skowronski D *et al*. 2011 Immunoepidemiologic correlates of pandemic H1N1 surveillance observations: higher antibody and lower cell-mediated immune responses with advanced age. *J. Infect. Dis.* **203**, 158–167. (doi:10.1093/infdis/jiq039)
32. Ma JL, Ma ZE. 2006 Epidemic threshold conditions for seasonally forced SEIR models. *Math. Biosci. Eng.* **3**, 161–172.
33. Cauchemez S, Valleron AJ, Boëlle PY, Flahault A, Ferguson NM. 2008 Estimating the impact of school closure on influenza transmission from Sentinel data. *Nature* **452**, 750–754. (doi:10.1038/nature06732)
34. Ionides EL, Bretó C, King AA. 2006 Inference for nonlinear dynamical systems. *Proc. Natl Acad. Sci. USA* **103**, 18 438–18 443. (doi:10.1073/pnas.0603181103)
35. Camacho A, Ballesteros S, Graham AL, Carrat F, Ratmann O, Cazelles B. 2011 Explaining rapid reinfections in multiple-wave influenza outbreaks: Tristan da Cunha 1971 epidemic as a case study. *Proc. R. Soc. B* **278**, 3635–3643. (doi:10.1098/rspb.2011.0300)
36. King AA, Ionides EL, Pascual M, Bouma MJ. 2008 Inapparent infections and cholera dynamics. *Nature* **454**, 877–879. (doi:10.1038/nature07084)
37. Skowronski DM *et al*. 2010 Prevalence of seroprotection against the pandemic (H1N1) virus after the 2009 pandemic. *Can. Med. Assoc. J.* **182**, 1851–1856. (doi:10.1503/cmaj.100910)
38. Sander B *et al*. 2010 Is a mass immunization program for pandemic (H1N1) 2009 good value for money? Evidence from the Canadian experience. *Vaccine* **28**, 6210–6220. (doi:10.1016/j.vaccine.2010.07.010)

Patterns of Spread of Influenza A in Canada

Daihai He, Jonathan Dushoff, Raluca Eftimie and David J.D. Earn

August 27, 2013 @ 15:18

6 Supplementary Material

6.1 Geographic locations of the ten Canadian provinces

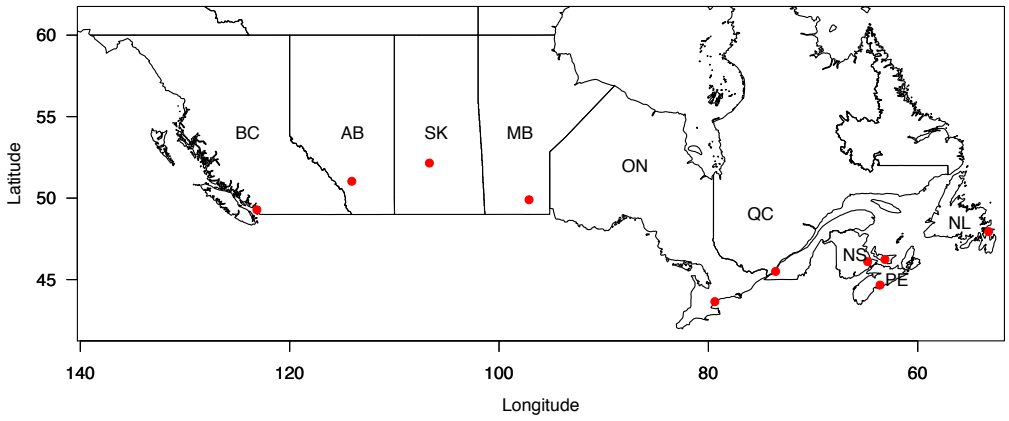

Figure S4: Geographic locations of the ten Canadian provinces. The red dot indicates the location of the most populous city in each province. AB, SK and MB are the *Prairie provinces*; NB, NS, PE and NL are the *Maritime provinces*.

6.2 p-values of four predictors in a generalized linear model

Figure S5 shows p-values associated with each of the four predictors and the four predictors taken together, while varying the threshold proportion of quantile time (see main text). We

compared two different temperature predictors: the number of days when the mean temperature was below zero between September and December (panel (a)), and the mean temperature in October (panel (b)). We found that the p-value associated with all four predictors together (curve A) is smaller using mean October temperature as the temperature predictor. Longitude rank (L) is a significant predictor in the *initial* stage of the epidemic (when the threshold proportion is less than 30%) for both temperature predictors (panels (a) and (b)); while the two climatic predictors, temperature (T) and humidity (H), are significant predictors (panel (b)). Humidity (H) and temperature (T) are significant predictors ($p < 0.05$) when the threshold proportion exceeds 20% (panel (b)). These results suggest that climatic variables likely influenced the spatial pattern of influenza A across Canada.

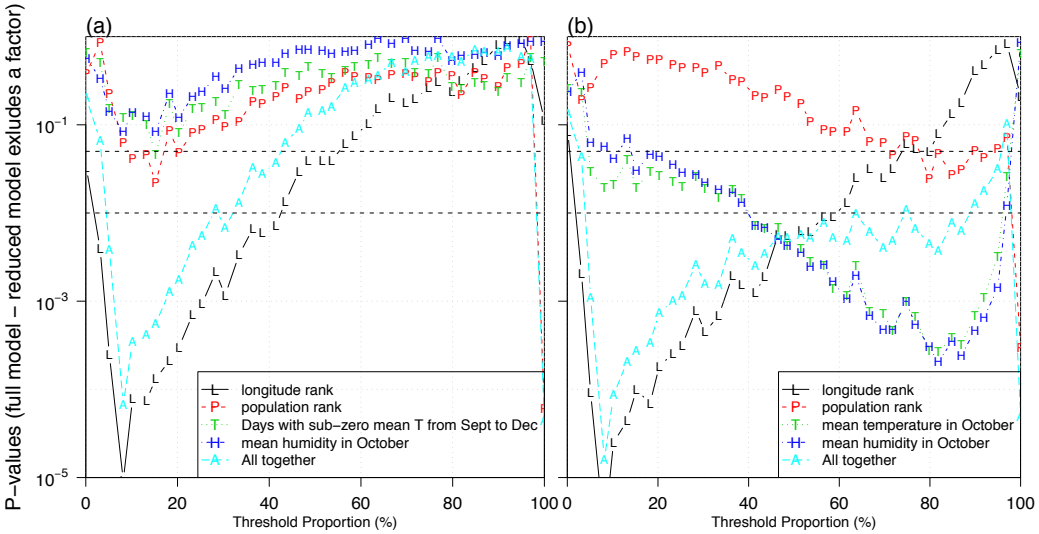

Figure S5: The impact of varying threshold proportion and temperature predictor on p-values associated with each of the four predictors and the four predictors taken together. (a) Temperature predictor is number of days when the mean temperature is below zero between September and December; (b) Temperature predictor is mean temperature in October. In each panel, the five curves show the p-values of longitude rank (demarcated by L), population rank (P), humidity (H), temperature (T), and all four together (A). Two horizontal dashed lines indicate the two levels of significance, 1% and 5%.

6.3 Direct comparison between longitude and population predictors

In the main text, we reported that longitude rank, humidity and temperature are significant predictors. Here we directly compare longitude rank and population rank. To test whether one predictor is better than the other, we reparameterized our model using standardized variables (we divided each variable by its standard deviation), and replaced the focal predictors with their sums and differences. This reparameterized model has a parameter measuring the difference between the absolute values of the partial correlation coefficients of the longitude rank and population rank; the p-value associated with this parameter was not significant, indicating that we do not have statistical evidence at the 5% level that longitude rank is a better predictor than population rank.

6.4 Comparing the spatial spreading pattern of seasonal epidemics versus the 2009 pandemic

Figure S6 compares the spatial spread of seasonal epidemics versus the 2009 pandemic. We first define the scaled cumulative incidence (laboratory-confirmation) curve (CIC). Given a time series of weekly laboratory confired cases for a season in a province, we calculate the cumulative sum series (`cumsum` in R), then divide by the total of number of confirmations for the given season in this province. For each of the seven regions (6 provinces and maritime mega-province), we calculate the CIC for each of the nine pre-pandemic seasons, and take an average for each province over the nine seasons. The averaged CIC for the pre-pandemic seasons is shown in panel (a). The CIC for the 2009 pandemic fall wave (August 2009 to August 2010) are shown in panel (b). We focus on the fall wave, excluding the spring wave, since the data for the spring wave contain a substantial proportion of seasonal strains, and the testing policy changed abruptly during the period. Figure S6 shows a striking similarity in the pattern of spatial spread of both the seasonal epidemics and the 2009 pandemic, from west to east.

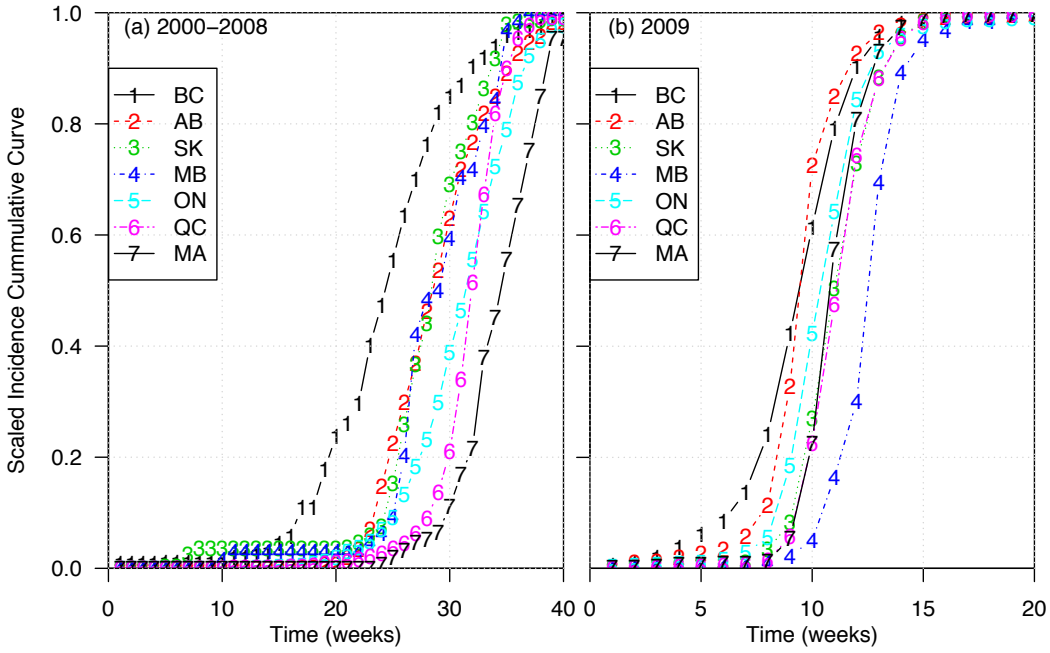

Figure S6: Comparison of the pattern of spatial spread of seasonal epidemics versus the 2009 pandemic. Panel (a) shows the scaled cumulative incidence curve (CIC), averaged over nine pre-pandemic seasons, for the seven regions. Panel (b) shows the CIC for the 2009 pandemic fall wave.

6.5 Comparison of three sub-models via AICc

Table S2 presents a comparison of the explanatory power of three sub-models using the second-order Akaike Information Criterion (AIC_c)[1, 2, 3]. Each of the models includes an increment in transmission when schools re-opened; the table reveals that the data for all regions (except for MB) are best explained by an additional effect of temperature variation. The differences among models including either of the two weather variables are marginal in ON and MB (*i.e.*, $\Delta AIC_c < 6$ [3]), indicating similar fits. Including neither weather variable yields a much worse fit.

6.6 Maximum likelihood estimates of parameters and simulations

Figure S7 shows (a) the total number of laboratory-confirmed influenza cases in each province during the pandemic year (with a box plot of annual cases during pre-pandemic seasonal epi-

Table S2: Comparison of three sub-models (see Methods). (i) Temperature variation only; (ii) humidity variation only; (iii) no climatic variation. All three models include reduced transmission when school is not in session. The table entries represent ΔAIC_c, *i.e.,* the difference between the AIC_c value for the best sub-model (which has the smallest AIC_c value) and the AIC_c value for each of the three sub-models. Thus, "best" indicates that the sub-model in the column in question yields the best fit for the region in question. Large ΔAIC_c values indicate a poor sub-model.

Province	**(i) Temperature (+ school term)**	**(ii) Humidity (+ school term)**	**(iii) None (but school term)**
BC	**best**	9.4	33.3
AB	**best**	16.5	34.4
SK	**best**	5.7	30.5
MB	1.0	**best**	16.4
ON	**best**	2.6	21.6
QC	**best**	8.3	31.8
MA	**best**	6.3	40.9

demics for comparison), (b) the reporting ratios estimated from the three sub-models for the pandemic year, and (c) the school term factor (increment in transmission due to school re-opening) estimated from the three sub-models for the fall wave of the 2009 pandemic. The sub-model without temperature or humidity (triangle for each province in panels (b,c)) tends to give a higher reporting ratio and higher school term factor than the other two sub-models, probably because this model does not fit as well.

Figure S8 shows the likelihood profiles for sub-model (i) as a function of temperature intensity (α_T) in each of the seven regions. These profiles show how the temperature intensity affects the fits. We also notice the similarity in the shape of the profile among the prairie provinces (AB, SK and MB), and between BC and ON, between QC and MA.

Figure S9 and Figure S10 compare the observed data to simulations of three sub-models in the seven regions. The simulations including weather variables match the observed data better than those without weather variables.

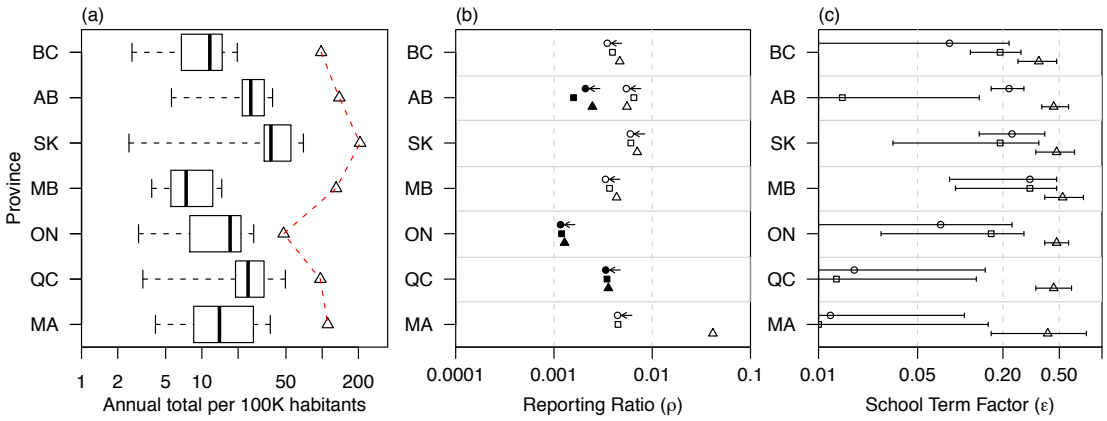

Figure S7: Influenza A case reports and model-estimated reporting ratios. (a) Annual lab-confirmed influenza A cases per 100,000 inhabitants (on a log scale) during the pre-pandemic seasons (boxplots) and during the 2009 pandemic (triangles). (b) The estimated reporting ratio (ρ) for the 2009 pandemic season, using three sub-models (see Methods); the filled symbols show the reporting ratio in provinces where testing restrictions were implemented, while the open symbols show the reporting ratio in provinces where testing restrictions were never imposed. Since in Alberta, testing restrictions were not applied until November 2009, we estimate ρ separately for before (open) and after (filled) restricted testing commenced. For each province, the three symbols (circle, square, and triangle, from top to bottom) correspond to sub-models (i)-(iii) as defined in Methods. Note that in provinces where testing restrictions were applied (i.e., AB, ON, QC), the reporting ratios were significantly lower than for the rest of the country. Arrows indicate the best sub-model. (c) The estimated school term factor (ε) for the 2009 pandemic season, using three sub-models, with whiskers indicating 95% confidence interval.

6.7 Effect of earlier or delayed vaccination

Vaccination against pH1N1 in Canada began in late October 2009, initially in vulnerable groups and by mid November in the entire population [8, 9]. The simulations summarized in Figure S9 and Figure S10 assumed, for simplicity, that vaccination began on 10 November 2009 in all provinces. Figure S11 summarizes the expected outcomes in terms of additional cases prevented (or caused) if vaccination had been initiated 1–3 weeks earlier (or later). Overall, earlier vaccination (panel a) would have had a substantially stronger effect than delayed vaccination (panel b). Earlier vaccination would have reduced incidence in all provinces, but would have had the smallest relative impact in AB, ON and BC, probably because the spring wave was larger in AB and ON [10]. The autumn wave began earlier in these provinces, and vaccine

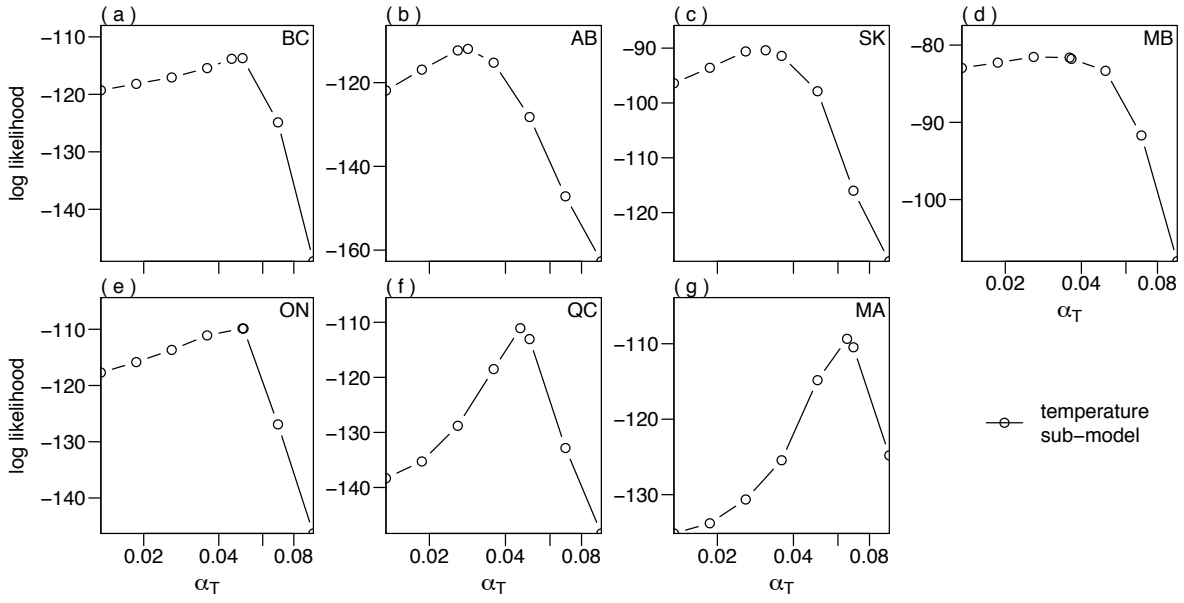

Figure S8: Likelihood profiles of sub-model (i) as a function of temperature intensity in each of the seven Canadian regions. The likelihood profile is obtained by maximizing the likelihood while fixing the intensity at a variety of values, via iterated filtering [4].

coverage was lowest in these provinces [11]. The four Atlantic provinces, as well as QC, MB and SK, would have benefited the most from an early vaccination program.

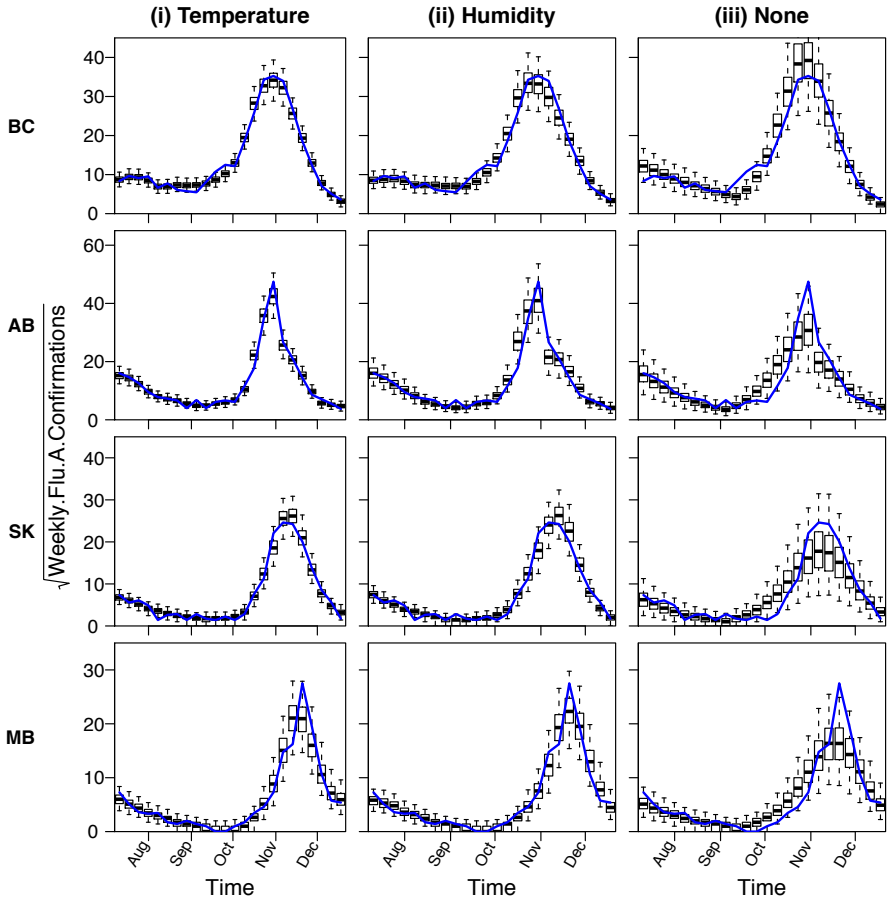

Figure S9: Simulations compared with observed pH1N1 influenza cases (blue) in four Canadian provinces (BC, AB, SK and MB) in 2009. Boxplots (Tukey-style with whiskers showing 2.5% and 97.5% quantiles) are based on 1000 stochastic simulations of the best model (Table S2); the stochastic version of each model was implemented using the Euler-multinomial approach [5, 6, 7] with a time step of one day; in simulations of provinces with small populations there were occasional fadeouts, so a single infection was introduced at these times to mimic transmission among provinces.

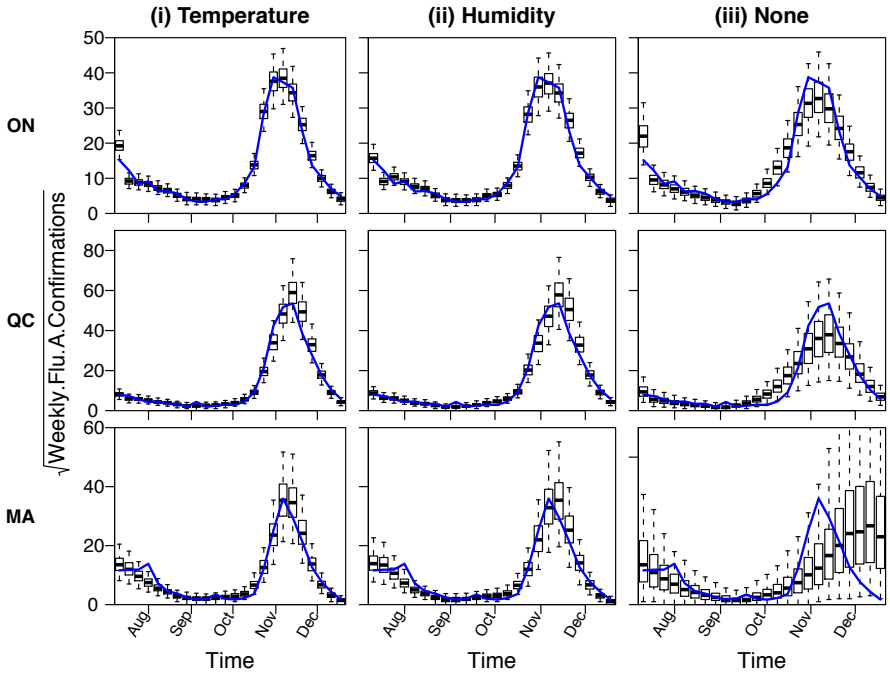

Figure S10: Simulations (boxplots) compared with observed pH1N1 influenza cases (blue) in two Canadian provinces (ON and QC) and the maritime mega-province (MA) in 2009.

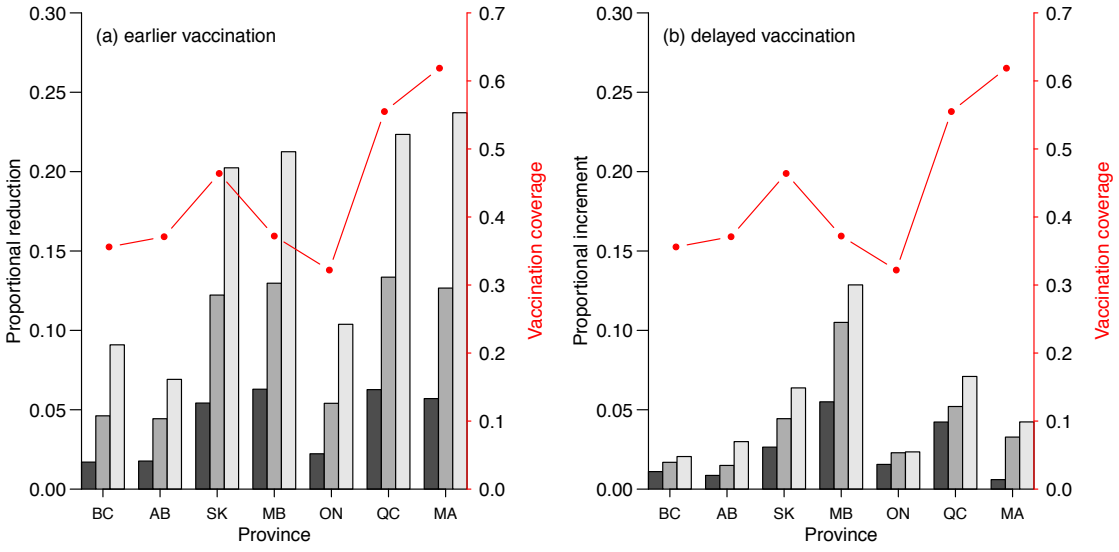

Figure S11: Predicted impact of earlier or later initiation of vaccination campaigns during the 2009 influenza pandemic, based on our best-fit transmission model for each region. (a) Estimated proportional **reduction** in the number of pH1N1 cases resulting from vaccine administration 1 (black bar), 2 (dark grey bar) or 3 (light grey bar) weeks **earlier**. (b) Estimated proportional **increase** in the number of pH1N1 cases resulting from vaccine administration 1 (black), 2 (dark grey) or 3 (light grey) weeks **later**. The thin red curves show the overall H1N1 vaccine coverage (i.e., proportion of population vaccinated) for each region. Note the higher vaccine coverage in SK and the maritime mega-province (MA), which could explain the higher impact of earlier vaccination on the reduction of cases in these provinces (panel a).

6.8 Assumption on initial susceptible proportion

In the main text, we assumed the initial susceptible proportion (on 4 July 2009) was 65% in all provinces. Results based on different assumptions, namely $S(0) = 0.8N$ and $S(0) = 0.4N$, are summarized in Tables S3–S6. Model comparisons based on these tables yield the same conclusions as reported in the main text. We found that a sub-model with temperature variation yields the smallest AICc in almost all provinces, except for MB (the difference is very small), thus we identified this sub-model as the best model. We also found that with a smaller $S(0)$, the estimated attack rate (AR) is closer to published values (20–30%) [12]. The estimated reporting ratio is also larger with a smaller $S(0)$. These results indicate that the pandemic H1N1 strain might not be as novel as the initial level of HI titers (using 1:40 as threshold) suggested [13, 12, 14]. There could be other mechanisms of (cross-) protection not measured by HI titers.

Table S3: Model comparison via AICc. We reproduce Table S2 with initial susceptible proportion $S(0) = 0.8N$ (where N is the population size).

Province	**(i) Temperature (+ school term)**	**(ii) Humidity (+ school term)**	**(iii) None (but school term)**
BC	**best**	9.2	33.6
AB	**best**	17.2	35.2
SK	**best**	5.7	31.6
MB	0.8	**best**	17.0
ON	**best**	0.3	19.9
QC	**best**	8.6	32.4
MA	**best**	5.3	38.9

Table S4: Maximum Likelihood Estimates of parameters from the best model. We reproduce Table 1 with initial susceptible proportion $S(0) = 0.8N$ (where N is the population size).

Province	$\mathcal{R}_e$	AR (%)	ρ	β_0	α_T	95% CI of α_T	ε	95% CI of ε
BC	1.27	53.4	0.0028	305.24	0.045	(0.033, 0.054)	0.088	(0.010, 0.247)
AB	1.25	52.2	0.0044	186.98	0.029	(0.023, 0.034)	0.247	(0.180, 0.325)
SK	1.33	56.1	0.0049	187.12	0.032	(0.022, 0.039)	0.261	(0.146, 0.484)
MB	1.32	56.2	0.0027	203.35	0.037	(0.013, 0.050)	0.363	(0.088, 0.614)
ON	1.30	55.3	0.0010	329.28	0.050	(0.035, 0.053)	0.075	(0.010, 0.261)
QC	1.27	55.9	0.0027	299.24	0.046	(0.042, 0.053)	0.018	(0.010, 0.162)
MA	1.30	57.5	0.0039	330.00	0.064	(0.055, 0.076)	0.012	(0.010, 0.113)

Table S5: Model comparison via AICc. We reproduce Table S2 with initial susceptible proportion $S(0) = 0.4N$ (where N is the population size).

Province	**(i) Temperature (+ school term)**	**(ii) Humidity (+ school term)**	**(iii) None (but school term)**
BC	**best**	9.4	33.0
AB	**best**	16.0	34.5
SK	**best**	5.5	30.1
MB	0.9	**best**	16.7
ON	**best**	5.8	25.2
QC	**best**	7.7	31.1
MA	**best**	6.8	41.0

Table S6: Maximum Likelihood Estimates of parameters from the best model. We reproduce Table 1 with initial susceptible proportion $S(0) = 0.4N$.

Province	$\mathcal{R}_e$	AR (%)	ρ	β_0	α_T	95% CI of α_T	ε	95% CI of ε
BC	1.27	26.7	0.0057	609.60	0.045	(0.032, 0.055)	0.088	(0.010, 0.247)
AB	1.25	26.5	0.0086	375.20	0.029	(0.022, 0.034)	0.247	(0.180, 0.343)
SK	1.32	28.2	0.0097	373.05	0.031	(0.020, 0.039)	0.261	(0.139, 0.484)
MB	1.33	28.5	0.0053	408.80	0.037	(0.013, 0.048)	0.384	(0.088, 0.614)
ON	1.28	27.6	0.0019	600.44	0.046	(0.034, 0.051)	0.092	(0.010, 0.275)
QC	1.26	27.7	0.0054	567.39	0.044	(0.042, 0.053)	0.038	(0.010, 0.234)
MA	1.35	29.6	0.0065	699.55	0.067	(0.062, 0.078)	0.010	(0.010, 0.154)

References

[1] He D, Dushoff J, Day T, Ma J, Earn DJD. Mechanistic modelling of the three waves of the 1918 influenza pandemic. Theoretical Ecology. 2011;4(2):283–288. 4

[2] Earn DJD, He D, Loeb MB, Fonseca K, Lee BE, Dushoff J. Effects of school closure on pandemic influenza incidence in Alberta, Canada. Annals of Internal Medicine. 2012;156(3):173–181. 4

[3] Camacho A, Ballesteros S, Graham AL, Carrat F, Ratmann O, Cazelles B. Explaining rapid reinfections in multiple-wave influenza outbreaks: Tristan da Cunha 1971 epidemic as a case study. Proceedings of the Royal Society, Series B, Biological Sciences. 2011;in press. 4

[4] Ionides EL, Bretó C, King AA. Inference for nonlinear dynamical systems. Proceedings of the National Academy of Sciences of the United States of America. 2006;103(49):18438–18443. 7

[5] Lloyd AL. Destabilization of epidemic models with the inclusion of realistic distributions of infectious periods. Proc Roy Soc Lond B. 2001;268:985–993. 8

[6] Bretó C, He D, Ionides EL, King AA. Time series analysis via mechanistic models. Annals of Applied Statistics. 2008;3(1):319–348. 8

[7] He DH, Ionides EL, King AA. Plug-and-play inference for disease dynamics: measles in large and small populations as a case study. J R Soc Interface. 2010;7(43):271–283. 8

[8] Hill K. H1N1 influenza update - province outlines immunization plans [news release on the internet cited by Dec. 22 2009]. Government of Saskatchewan News Release. 2009;Available from: `http://www.gov.sk.ca/news?newsId=96b0757b-c725-4f6d-9b2a-d40e18b55f92`. 6

[9] ServiceCanda. Ontario announces flu shot rollout for seasonal and H1N1 vaccines [news release on the internet cited by Dec. 22 2009]. Government of Ontario News Release. 2009;Available from: http://www.news.ontario.ca/mohltc/en/2009/09/ontario-announces-flu-shot-rollout-for-seasonal-and-h1n1-vaccines.html. 6

[10] FluWatch. FluWatch reports 1999/2000 – 2009/2010. Public Health Agency of Canada. 2010;Available from: http://www.phac-aspc.gc.ca/fluwatch. 6

[11] Gilmour H, Hofmann N. H1N1 vaccination. Statistics Canada Health Reports. 2010;82-003-X. Available from: http://www.statcan.gc.ca/pub/82-003-x/2010004/article/11348-eng.htm. 7

[12] Kelly H, Peck HA, Laurie KL, Wu P, Nishiura H, Cowling BJ. The age-specific cumulative incidence of infection with pandemic influenza H1N1 2009 was similar in various countries prior to vaccination. PLoS One. 2011;6(8):e21828. 11

[13] Hancock K, Veguilla V, Lu X, Zhong W, Butler EN, Sun H, et al. Cross-reactive antibody responses to the 2009 pandemic H1N1 influenza virus. N Engl J Med. 2009;361:1945–1952. 11

[14] Skowronski DM, Hottes TS, Janjua NZ, Purych D, Sabaiduc S, Chan T, et al. Prevalence of seroprotection against the pandemic (H1N1) virus after the 2009 pandemic. Canadian Medical Association Journal. 2010;182(17):1851–1856. 11